eNeuro

Research Article: Methods/New Tools | Novel Tools and Methods

Targeting morphine-responsive neurons: generation of a knock-in mouse line expressing Cre recombinase from the mu opioid receptor gene locus

https://doi.org/10.1523/ENEURO.0433-19.2020

Cite as: eNeuro 2020; 10.1523/ENEURO.0433-19.2020

Received: 17 October 2019
Revised: 23 March 2020
Accepted: 9 April 2020

Manuscript title: Targeting morphine-responsive neurons: generation of a knock-in mouse line expressing Cre recombinase from the mu opioid receptor gene locus.

Abbreviated Title: Generation of a knock-in mu opioid receptor-Cre

Author Names and Affiliations:

Julie Bailly[1], Natalie Del Rossi[1], Léonie Runtz[1], Jing-Jing Li[1], DaWoon Park[1], Grégory Scherrer[2], Arnaud Tanti[1], Marie-Christine Birling[3], Emmanuel Darcq[1], Brigitte L Kieffer[1]

[1] Department of Psychiatry, McGill University, Douglas Hospital Research Center, Perry Pavilion Room E-3317.1, 6875 boulevard LaSalle, Montreal, QC H4H 1R3, Canada
[2] UNC Neuroscience Center, University of North Carolina, Chapel Hill NC 27599 USA
[3] CELPHEDIA, PHENOMIN, Institut Clinique de la Souris (ICS), Illkirch-Graffenstaden, 67404, France

Author Contributions: JB, ED and BLK designed the study; MCB, GS and BLK designed the knock-in mice strategy; MCB generated the mice; DWP performed animal care and genotyping; JB, NDR, LR, JJL, AT acquired the data; JB, ED and BLK performed the analysis, interpreted data and wrote the manuscript. All authors read and approved the submitted version.

Correspondence: brigitte.kieffer@douglas.mcgill.ca

Figures: 3
Extended Data: 2
Tables: 0
Multimedia: 1

Abstract: 250
Significance Statement: 85
Introduction: 410
Discussion: 390

Acknowledgements: We thank the staff at the animal facility of the Neurophenotyping Center and the Molecular and Cellular Microscopy Platform of the Douglas Mental Health University Institute (Montréal, Canada) for microscope usage. We thank Kai-Florian Storch and Lei Zhu for technical support. We also thank the Mouse Clinic Institute (Illkirch, France) for generating *Oprm1*-Cre mice. The NIDA Supply Drug Program generously provided morphine.

Conflict of Interest: The authors declare no competing interest.

Funding sources: This work was supported by National Institute of Health (National Institute of Drug Abuse Grant No. DA05010 to BLK and National Institute on Alcohol Abuse and Alcoholism, Grant No. 16658 to BLK), the Canada Fund for Innovation and the Canada Research Chairs to ED and BLK, and by the Wallonie-Bruxelles International (JB).

Targeting morphine-responsive neurons: generation of a knock-in mouse line expressing Cre recombinase from the mu opioid receptor gene locus.

Abstract

The mu opioid receptor (MOR) modulates nociceptive pathways, reward processing, and mediates the strong analgesic and addictive properties of both medicinal as well as abused opioid drugs. MOR function has been extensively studied, and tools to manipulate or visualize the receptor protein are available. However, circuit mechanisms underlying MOR-mediated effects are less known, because genetic access to MOR-expressing neurons is lacking. Here we report the generation of a knock-in *Oprm1*-Cre mouse line, which allows targeting and manipulating MOR opioid-responsive neurons. A cDNA encoding a T2A cleavable peptide and Cre-recombinase fused to enhanced green fluorescent protein (eGFP/Cre) was inserted downstream of the *Oprm1* gene sequence. The resulting *Oprm1*-Cre line shows intact *Oprm1* gene transcription. MOR and eGFP/Cre proteins are co-expressed in the same neurons, and localized in cytoplasmic and nuclear compartments, respectively. MOR signaling is unaltered, demonstrated by maintained DAMGO-induced G protein activation, *and in vivo* MOR function is preserved as indicated by normal morphine-induced analgesia, hyperlocomotion and sensitization. The Cre-recombinase efficiently drives expression of Cre-dependent reporter genes, shown by local-virally-mediated expression in the medial habenula and brain wide fluorescence upon breeding with tdTomato reporter mice, the later showing a distribution patterns typical of MOR expression. Finally, we demonstrate that optogenetic activation of MOR neurons in the ventral tegmental area of *Oprm1*-Cre mice evokes strong avoidance behavior, as anticipated from the literature. The *Oprm1*-Cre line is therefore an excellent tool for both mapping and functional studies of MOR-positive neurons, and will be of broad interest for opioid, pain and addiction research.

Significance Statement

Here we develop an innovative tool to characterize circuit mechanisms underlying opioid actions, which may help the research communities to improve the knowledge on circuitry adaptation and response to opioid. The tool is particularly relevant in the context of the current opioid crisis. Medicinal and abused opioids act primarily on Mu Opioid Receptor (MOR) and we developed here a Cre mouse line to specifically target and manipulate MOR-expressing neurons. This resource is with huge potential for mapping, molecular characterization and functional studies of opioid-responsive neurons.

Keywords

Oprm1 gene; knock-in mice; Cre-loxP system; cell-specific gene targeting; morphine; enkephalins

Introduction

The mu opioid receptor (MOR) is the primary molecular target for medicinal and abused opioids. This receptor mediates both the unrivalled analgesic properties of opioids for pain treatment, and their adverse effects including notably their strong addictive potential (Matthes et al., 1996; Darcq et al., 2018), which is driving the current opioid epidemic (World Health Organization, 2017; Volkow et al., 2019). Under physiological conditions, MOR is activated by endogenous opioid peptides and modulates nociceptive pathways (Corder et al., 2018), respiration centers (Levitt et al., 2018) and brain circuits that process reward and emotions (Contet et al., 2004; Lutz et al., 2013). Although the essential role of MOR in pain, drug abuse and mood disorders is well established, and receptor adaptations to chronic opioids have been well studied at cellular level (Williams et al., 2013; Cahill et al., 2016), circuit mechanisms underlying MOR function (Darcq & Kieffer, 2018), and the regulation of neuronal communication driven by MOR (Mechling et al., 2016) and MOR agonists (Nasseef et al., 2019), are poorly understood.

Several genetic mouse tools have been developed to study MOR function, but have not given genetic access to MOR-expressing neurons as yet. A knock-in MOR-mCherry mouse line was developed to map MOR protein expression throughout the nervous system brain (Gardon et al., 2014; Erbs et al., 2015), and allows speculating about circuit mechanisms driving MOR-mediated behaviors. Mice with a floxed *Oprm1* gene have permitted receptor deletion in targeted neurons from nociceptive (Weibel et al., 2013) and reward (Charbogne et al., 2017) pathways, uncovering some circuit mechanisms of MOR-mediated pain control and motivation. A next step to understand MOR physiology, and to fully investigate neural dysfunctions associated to opioid drug use, misuse and abuse, is to study and manipulate the activity of MOR-expressing neurons that directly respond to both exogenous and endogenous mu opioids.

To this aim, a best approach is to create a mouse line expressing the Cre recombinase in MOR-expressing neurons. Here we report the generation of a line expressing the Cre recombinase under the control of the *Oprm1* gene (encoding MOR) promoter, and present molecular and behavioural characterization of this mouse line (*Oprm1*-Cre line). We also show successful labeling of MOR-positive neurons using a fluorescent Cre-dependent reporter mouse line. We finally demonstrate that optogenetic stimulation of MOR-positive neurons in the ventral tegmental area is sufficient to induce strong avoidance behaviour, as anticipated from the literature. The line fulfills all the criteria to successfully study and manipulate MOR neurons.

Materials and methods

Animals

The *Oprm1*-Cre knock-in mouse line was generated by homologous recombination to express a Cre recombinase under the control of the *Oprm1* promoter. In these mouse line, a cDNA encoding a functional eGFP/Cre-recombinase fusion protein was inserted into the exon 4 of the MOR gene, in frame and 5' of the stop codon, as described in (Gardon et al., 2014; Erbs et al., 2015). The eGFP/Cre cDNA was generated by cloning the Cre cDNA (gift from Daniel Metzger, IGBMC, Illkirch, France) by PCR into the BglII and EcoRI sites of the pEGFP-C2 plasmid (Clontech/Addgene), resulting in a 7 amino acid linker SGRTQIS between the two proteins. The cloning of Cre in 3' in phase with eGFP and the absence of mutations were verified by DNA sequencing. The functionality of the eGFP/Cre fusion protein was verified by co-transfecting COS cells with this eGFP/Cre plasmid and with the Cre activity reporter plasmid pCMV-LneoL-Betagal (gift from Daniel Metzger, IGBMC, Illkirch, France). Further, a T2A cleavable peptide sequence (Szymczak et al., 2004) was inserted, joining the *Oprm1 gene* to the eGFP/Cre sequence, so that the eGFP/Cre enzyme is released from the receptor upon translation of the MOR-T2A-eGFP/Cre fusion protein. The entire construct was verified by DNA sequencing

before homologous recombination was performed. We then verified that the construct had not integrated randomly in the genome. Of note, no DNA sequencing or splicing analysis of the *Oprm1* gene was later performed in *Oprm1*-Cre mice. The genetic background of all mice was 100% C57BL/6N. Mice were group-housed (maximum fives mice/cage) in a temperature and humidity-controlled animal facility (21±2°C, 45±5% humidity) on a 12-h dark-light cycle with food and water ad libitum. All experiments were performed in accordance with the Canadian Council of Animal Care and by the Animal Care Committees.

Genotyping PCR

For routine genotyping, the forward primer is: ATATTATTTTCCCTGACGCGTTCTG and the reverse primer is: CTGAAGATTGACATTGTATCGAGGA. The PCR product for the *Oprm1*-Cre wild-type allele is 311 bp and for the *Oprm1*-Cre knock-in allele is 387 bp. See **Extended Data Figure 1-1**.

Dissection for mRNA and signalling testing

Mice were sacrificed by dislocation and the whole brain was quickly extracted and placed upside down in a chilled metal matrix (ASI instruments, Warren, MI, USA). Cold razor blades were inserted into the 1-mm-spaced coronal groove with the first most rostral one inserted at the limit of olfactory bulbs. Brain punches were dissected using 1 or 2 mm tissue corers and placed into microtubes, rapidly frozen and stored at -80°C. Half brain was used to prepare striatal membranes incubated with different doses of DAMGO in [^{35}S]-GTPγS assay. The other half brain was used to extract RNA in 8 regions : DS, dorsal striatum; NAc, nucleus accumbens; Hb, habenula; IPN, interpeduncular nucleus; VTA/SN, ventral tegmental area/substantia nigra; Cer, cerebellum; PAG, periaqueductal gray; SC, spinal cord, and the gene expression was examined by qPCR.

Quantitative analysis of transcript expression

RT-qPCR was adapted from (Meirsman et al., 2016). 600 ng of RNA was reverse transcribed using the M-MLV Reverse Transcriptase Kit (Invitrogen) according to the manufacturer's instructions. The cDNA was subjected to 45 cycles of amplification using LightCycler 480 SYBR I Green Master Mix (Roche) in the LightCycler 480 II Real-Time PCR System (Roche). cDNA samples were loaded in triplicate and a no-template control (NTC) reaction, with just water, was included to check for non-specific amplification. Relative fold changes were calculated by the comparative Ct method ($2^{-\Delta\Delta CT}$) (Livak et al., 2001) using B2M as housekeeping gene.

mRNA In situ Hybridization

In situ hybridization was performed using Advanced Cell Diagnostics RNAscope® probes and reagents (Hayward, CA, USA) according to the manufacturer instruction) to detect mRNA encoding MOR (*Oprm1*) and eGFP (*EGFP*). Briefly, *Oprm1*$^{+/+}$ and *Oprm1*$^{Cre/Cre}$ male mice were sacrificed and fresh brains were flash-frozen in isopentane. The 10-µm thick coronal sections were cut using a cryostat (Leica), directly mounted on superfrost slides and kept at -80°C until processing. Sections were first fixed in chilled 10% neutral buffered formalin for 15 mins at 4°C, dehydrated by increasing gradient of ethanol bathes and left to air dry for 5 minutes. Endogenous peroxidase activity was quenched with hydrogen peroxide reagent for 10 minutes, followed by protease digestion for 30 minutes at room temperature. The following sets of probes were then hybridized for 2 hours at 40°C in a humidity-controlled oven (HybEZ II, ACDbio): *EGFP*-C1 target region 2-707 (cat. No. 538851) and *Oprm1*-C2 target region 1135-2162 (cat. No. 315841-C2). Probes for *Oprm1*, and *eGFP* were revealed using respectively Opal Dye 520 and Opal Dye 570-labeled probes. Slides were then coverslipped with Vectashield mounting medium with DAPI for nuclear staining (Vector Laboratories) and kept at 4°C until imaging.

[^{35}S]-GTPγS binding assays

The assay was performed as previously described by (Pradhan et al., 2009; Erbs et al., 2015; Meirsman et al., 2016) on membrane preparations from striatum. Striatum was dissected following mouse cervical dislocation, placed on dry ice and store at -80°C. To evaluate the MOR function, striatum (n=2 pools x 4 per genotype) were pooled together and membranes were prepared by homogenizing tissues in 0.25M sucrose with a Polytron, followed by a centrifugation at 2500 rpm for 10 min at 4°C. Samples were diluted in TMEN (Tris 50 mM, MgCl2 3 mM, EGTA 0.2 mM, NaCl 100 mM, pH 7.4) followed by an ultracentrifugation at 40,000g for 30 min at 4°C (MLA-55 rotor). The membrane pellet was re-suspended in 0.32M sucrose by 10 strokes with a potter. Membrane preparations were diluted in 800 µl, aliquoted and stored at -80°C. Protein concentration was determined by the Bradford assay using a standard curve of Bovine Serum Albumin (BSA) and triplicate dilution of each sample. For each [^{35}S]-GTPγS binding assay, 5ug of protein was used per well. Samples were incubated with variable concentration of (3 10^{-9} to 2 10^{-10} M) of DAMGO in assay buffer containing 5mM GDP and 0.1nM [^{35}S]-GTPγS for 1 h at 25°C. After wash and filter steps, bound radioactivity was quantified using the liquid scintillation counter, (TopCount, Perkin Elmer). Non-specific binding was determined in absence of agonist. Basal activity was determined in the presence of 10 µM GTPγS. Calculations and sigmoidal dose-response binding curves were done using GraphPad PRISM 6 (GraphPad Software, Inc, USA).

Tissue preparation and immunohistochemistry

Mice were anesthetized with i.p. injections of 100 µl/100 g of a cocktail containing Ketamine/Xylazine/Acépromazine. An intra-cardiac perfusion was performed with ~10 ml ice-cold 1x phosphate buffered saline (PBS, Invitrogen) pH 7.4 followed by ~50 ml ice-cold 4%

paraformaldehyde (PFA, Electron microscopy sciences) using a peristaltic pump at ~10 ml/min. Brain were removed and post-fixed 24h at 4°C in the 4% PFA solution, cryoprotected at 4°C in 30% sucrose (Fisher Scientific) for 48h, embedded in OCT (Maker) frozen and finally store at -80°C. Brain were sliced into 30 µm coronal and sagittal sections using a cryostat (Leica) and sections were stored at 4°C in phosphate buffered saline (PBS). Immunohistochemistry was performed by washing the sections 3 x 10 in PBS, then 3 x 10 min with PBS/Triton-X-100 0,1% (PBS-T, Sigma), followed by 1h in a blocking buffer (PBS, 3% normal donkey serum NDS, Triton-X-100 0,2%), each at room temperature with gentle agitation. Sections were incubated overnight at 4°C with the following primary antibodies: 1:2000 anti-green fluorescent protein (Novus, NB100-1614, RRID: AB_523902), or with 1:1000 anti-MOR antibody (UMB3, Abcam, ab134054)**,** or with 1:1000 anti-dsred (Clontech, 632496, RRID: AB_10013483), or with 1:1000 anti-tyrosine hydroxylase (Abcam, ab112, RRID: AB_297840) in blocking buffer. Sections were then washed 3 x 10 in PBS-T, incubated for 2h at room temperature with appropriate AlexaFluor-conjugated secondary antibodies. Sections were washed 3 x 10 min in PBS-T with gentle agitation, placed in PBS and mounted on to glass slides with Moviol (PolyScience) and 4',6-diaminido-2-phenylindole (DAPI, ThermoFisher, 0.5 µg/ml, RRID:AB_2307445). The UMB3 MOR antibody showed no staining in sections from MOR knockout mice (**Extended Data Figure 1-2**).

Image acquisition

Slides were scanned on the Olympus VS120 (Olympus Corporation, Shinjuku, Tokyo, Japan) with a 10x objective. For fluorescence microscopy, an Olympus IX73 with 10x or oil immersion 60x objective was used. For confocal microscopy imaging, an Olympus FV1200 with 20x or oil immersion 60x objective, was used to take Z-stack images.

Behavioral experiments

242 *Morphine-induced analgesia.* Mice were intraperitoneally injected 2,5 or 5 mg/kg morphine or
243 saline and analgesia was tested using tail immersion (Erbs et al., 2015). Briefly, the mouse was
244 maintained in a cylinder and the tail was immersed in a water bath set at 48°C with a cut-off
245 time of 15s. Mice were allowed to recover for 1 min followed by a tail immersion in a second
246 water bath set at 52°C with a cut-off time of 10s. The baseline responding was measured for tail
247 flick before the first injection and the morphine-induced analgesia tests were performed 45 min
248 after the injection.
249
250 *Morphine-induced locomotor sensitization.* Locomotor activity was measured in Plexiglas activity
251 boxes (20 × 20 × 20 cm) surrounded by horizontal and vertical infrared sensor beams and
252 assisted by VersaMax software. To evaluate the morphine-induced hyperlocomotion at the first
253 session, mice were allowed to explore the boxes for 1h. Mice were then injected with saline
254 (1ml/kg) and returned to the boxes for 1h followed by an intraperitoneal injection of morphine
255 (40 mg/kg) or saline and activity was recorded for 2h. For locomotor sensitization, mice were
256 injected twice week with saline and placed in the boxes for 1h followed by morphine (40mg/kg)
257 injection and activity was recorded for 2h. Measurements were taken on day 1, 4, 8, 11, 14, 18
258 adapted from (Darcq et al., 2012).
259
260 *Stereotaxic surgery.* Animals were anesthetised with 5% isoflurane for 5 min and maintained at
261 2% isoflurane. For viral Cre-recombination, adult *Oprm1*$^{Cre/Cre}$ male mice were injected
262 unilaterally with 100 nl of AAV2.EF1a.DIO.mCherry (RRID: Addgene_20299) in the MHb (AP: -
263 1,35 ; ML: -0,25 ; DV: -2,8). For optogenetic experiment, adult *Oprm1*$^{Cre/Cre}$ male mice were
264 injected unilaterally with 400 µl of AAV2.EF1a.DIO.ChR2-mCherry (RRID: Addgene_20297) or
265 AAV2.EF1a.DIO.mCherry in the VTA (AP: -3.3, ML: -0.5, DV: -4.3). Two weeks after virus
266 injection, fiber-optic ferrules (200µm, NA: 0.37) were implanted above the VTA (AP: -3.3, ML: -
267 0.5, DV: -4.1). The implant was secured using a first layer of Metabond followed by a layer of

dental. Mice were allowed to recover for at least 4 weeks after infusion of virus before habituation to the optic cord and behavioral testing. The injected and implanted mice are designated as *Oprm1*-Cre $^{VTA\text{-}VTA::ChR2.}$

Real time place preference. Five weeks after the viral injections, mice were placed in a custom behavioral arena (black plexiglass 50 × 50 × 25 cm) divided into 2 identical chambers and allowed to explore each of two chambers for 20 min. Using an Anymaze hardware controller connected to the laser, light stimulation (473 nm, 10 mW) at 0, 10, 20 or 40 Hz (10 ms pulse width) was delivered through fiber-optic implants during the duration of their time spent in the light stimulation chamber. Mice received no light stimulation in the "no stimulation" chamber. At the start of the session, the mouse was placed in the non-stimulated side of the chamber. The percentage of time spent on paired stimulation side was recorded via a CCD camera interfaced with the Anymaze (Stoelting) software.

Statistical analysis

All data are presented as mean SEM. Statistical analysis was assessed using t tests or repeated-measures ANOVA. When ANOVA reached significance, a Tukey's honestly significant difference test was conducted. Non- significance was defined as $p>0.05$ and significance as $*p<0.05$, $**p<0.01$ and $***$ $p<0.001$.

Results

Unsuccessful attempts to develop transgenic mouse lines using both short and BAC promoters of the mu opioid receptor gene (*Oprm1*), led us to use homologous recombination to insert the Cre recombinase gene into the *Oprm1* gene locus. A knock-in strategy for the *Oprm1* gene was designed **(Figure 1a)** to generate a large precursor protein, which would be further

cleaved to release both the native MOR protein and a functional eGFP/Cre recombinase in cells that normally express the MOR. This approach produced the *Oprm1*$^{Cre/Cre}$ (or *Oprm1*-Cre) mouse line, which we characterized extensively.

We first tested whether insertion of the T2A-eGFP/Cre cDNA into the *Oprm1* gene locus modifies levels of gene transcription. Quantitative mRNA analysis in several brain regions, including most MOR-enriched regions, revealed that the genomic modification does not disrupt *Oprm1* transcription (**Figure 1b**). Using eGFP primers, we also detected the *egfp* transcript in *Oprm1*$^{Cre/Cre}$ but not *Oprm1*$^{+/+}$ control mice, suggesting that the entire *Oprm1-T2A-eGFP/Cre* transcript is transcribed in the knock-in line (not shown). We further performed double *in situ* hybridization using separate probes for *Oprm1* and *eGFP/Cre* mRNAs in brain sections from *Oprm1*$^{Cre/Cre}$ mice (2 mice, 8 sections), and found co-localization of the two transcripts in all the sections examined (**Figure 1c** at the level of striatum).

Second, we examined expression of MOR and eGFP/Cre proteins using immunohistochemistry in brain sections from heterozygous *Oprm1*$^{Cre/+}$ mice. In the medial habenula (MHb), i. e. the best MOR-enriched region, we observed predominant expression of the two proteins in both basolateral and apical subregions (**Figure 1d,** left panel**)** as expected (Gardon et al., 2014). Higher magnification (**Figure 1 d**, right panels) showed distinct subcellular distribution of the two proteins, as expected from the natural localization of MOR (cytoplasm/membrane) and eGFP/Cre (nuclear). The latter observation suggests that the T2A-eGFP/Cre fusion protein was mostly cleaved, which was further supported by western blot (not shown) and the expected activity for the two proteins (below).

Third, we investigated whether MOR function is intact in this mouse line. We tested MOR signalling in response to DAMGO, a MOR-selective agonist. The [^{35}S]-GTPγS binding assay showed similar potency and efficacy of DAMGO in samples from the two genotypes, suggesting that MOR-mediated G protein activation is intact in the *Oprm1*-Cre line **(Figure 1e**). Next we compared two best-documented *in vivo* effects of morphine in *Oprm1*$^{Cre/Cre}$ and

Oprm1$^{+/+}$ mice. Morphine-induced hyperlocomotion, as well as locomotor sensitization were measured in *Oprm1*$^{Cre/Cre}$ and *Oprm1*$^{+/+}$mice (**Figure 1f).** A two-way, mixed design ANOVA, with genotype as a between subjects-factor, and days since injection as a within subjects-factor, indicated a main effect only for days, Fs (5, 60) = 35.19, ps < 0.001. The interaction term was not significant, F (5, 60) = 1,70, p>0.05. Pairwise comparisons tests were performed using a Tukey's honestly significant difference test. The mean total traveled distance at day 11, 14 and 18 was significantly higher compared to day 1, 4 and 8 (ps <0.001), and day 8 was significantly higher than day 1 (ps <0.05). Morphine therefore induced similar hyperlocomotion and sensitization in the two genotypes. Morphine analgesia was assessed using the tail immersion test (**Figure 1g**). At 48°C, a two-factor (genotype x injection treatment) between subject ANOVA yielded significant main effects for injection treatment, $Fs_{(2,\ 54)} > 53.77$, ps < .0001. The interaction term was not significant, $F_{(2,54)} = 1.724$, p > .05. Tukey's honestly significant difference tests computed on the main effect for treatment indicated that the mean tail withdrawal latencies were significantly increased for both genotypes and at 2,5 mg/kg and 5 mg/kg morphine doses (all ps<0.001). Similarly at 52°C, a two-factor (genotype x injection treatment) between subject ANOVA yielded significant main effect for the treatment, $Fs_{(2,\ 51)} >$ 45.32, ps < .0001, with no significant interaction ($F_{(2,51)} = 0.453$, p > .05). Tukey's honestly significant difference tests indicated that mean tail withdrawal latencies were significantly increased for the two genotypes and at the two morphine doses (all ps<0.001). Together results show intact morphine effects on both activity and pain perception in mutant mice, and overall the data suggest that MOR signalling and function *in vivo* are maintained in the *Oprm1*-Cre line.

Fourth, we examined whether the eGFP/Cre fusion protein is able to mediate Cre/LoxP recombination in the *Oprm1*-Cre line. Of note, although the eGFP/Cre fusion has the advantage of allowing detection of the recombinase, non-eGFP fluorophores should be used when combining with other reporters. We therefore used red fluorescent reporters in the subsequent experiments. We first injected a Cre-dependent fluorescent reporter AAV2-mCherry virus in the

MHb, and found a strong fluorescent signal (**Figure 2a,** left) with a pattern similar to the eGFP/Cre signal (**Figure 1c)** in apical and basolateral MHb. Several compartments of the interpeduncular nucleus (IPN) were also strongly labelled, indicating that the fluorescent reporter is transported along fibers to the major projection site (**Figure 2a,** left), as expected (Gardon et al., 2014). To get a brain-wide view of Cre-mediated recombination in the *Oprm1*-Cre line, we crossed the mice with Cre-dependent reporter Rosa^{lsltdTomato} mice (see methods). The tdTomato protein was strongly expressed in MHb, fasciculus retroflexus and IPN **(Figure 2a,** right**),** with a pattern similar to that observed upon Cre-dependent viral reporter expression except that areas out of the MHb-IPN pathway were also labelled. In particular, fluorescence was observed throughout the mesolimbic pathway, including striatal patches, direct pathway projections neurons and the ventral tegmental area (VTA)/substantia nigra typical of MOR expression (Cui et al., 2014). Recombination also occurred in the central amgydala, intercalated amygdala and the endopiriform nucleus, but not in the basolateral amygdala, concordant with sites of high MOR expression (Erbs et al., 2015). Together these anatomical data demonstrate that the eGFP/Cre protein is functional. Further, Cre activity is found at known sites of MOR expression, indicating accurate transcriptional control of *Cre-egfp* under the *Oprm1* promoter. Staining patterns observed here differ from those previously reported in MOR-mCherry mice (Gardon et al., 2014; Erbs et al., 2015), as two distinct knock-in strategies were used in order to label either MOR-expressing cells (MOR-Cre mice, this study) or the receptor itself (MOR-mCherry mice).

Finally, we tested whether *Oprm1*$^{Cre/Cre}$ mice can be used for cell specific optogenetic manipulation of MOR-neurons. Earlier studies have demonstrated that optical stimulation of GABAergic interneurons in the VTA induces avoidance behaviour, as a consequence of dopamine (DA) neuron inhibition (Tan et al., 2012). MOR is a Gi-coupled receptor expressed in these interneurons, and a best-known mechanism for MOR-mediated reward is through inhibition of these VTA GABA interneurons, an activity that in turn disinhibits DA neurons

(Johnson et al., 1992; Fields et al., 2015). We therefore hypothesized that optogenetic activation of MOR-eGFP/Cre-expressing neurons in the VTA of *Oprm1*$^{Cre/Cre}$ mice would produce a place avoidance, as did the stimulation of the entire population of VTA GABAergic neurons in the Tan et al study. We injected a Cre-dependent AAV2-channelrhodopsin virus in the VTA (**Figure 3a-b**) to express ChR2 mainly in MOR/GABAergic interneurons **(Figure 3c)** and tested animals using a real time place-testing (RTPT) paradigm **(Figure 3d).** A two-way ANOVA with virus as between subject-factor and frequency as within subject-factor yielded a significant interaction ($F_{(3,51)}$ = 16.93, p<0.001). Simple effect test revealed that the *Oprm1*-Cre$^{VTA\text{-}VTA}$::ChR2 mice spent significantly less time on the side paired with light-stimulation than control mice at 10 Hz (**p<0.01), 20 Hz and 40 Hz (***p<0.001) compared to control mice **(Figure 3d-e),** indicating that optical stimulation triggered place avoidance. The stimulation did not affect total activity measured at 20Hz (unpaired t-test, t(14) = 1.497, p>0.05) (**Figure 3f).** Together, data demonstrate that activation of MOR-positive neurons in the VTA produce avoidance, as predicted. The *Oprm1*-Cre line, therefore, efficiently drives Cre-mediated recombination to modulate behaviour.

Discussion

Originally developed to allow gene targeting in specific cells using Cre/LoxP recombination (Gaveriaux-Ruff et al., 2007), Cre driver lines are also extensively used to label specific neuronal populations and visualize their connectivity patterns when combined with Cre-dependent fluorescent reporter mouse lines or viruses, (D. Cai et al., 2013; Soden et al., 2014), or to monitor the activity of phenotypically defined neuronal ensembles using Cre-dependent calcium indicators (Russell, 2011). The utility of mouse Cre lines has further expanded with the advent of optogenetic and chemogenetic approaches, which allow manipulating Cre-expressing neurons to understand circuit mechanisms underlying behaviour (Fenno et al., 2011; Sternson

et al., 2014). Transgenic Cre lines have now been generated by individual laboratories, as well as large initiatives, including the GENSAT program (Gong et al., 2007) the NIH Blueprint Cre driver Network (Taniguchi et al., 2011) and the Allen Brain Institute .

Lines providing access to the opioidergic circuitry remain limited (reviewed in (Darcq & Kieffer, 2018)), and targeting cells responding to medicinal and abused opioid drugs is a desirable goal. To study opioid peptide-expressing cells, Cre lines using *Pdyn*, *Penk* and *Pomc* gene promoters have been created (see (Harris et al., 2014) for *Penk* and *Pomc* lines), and *Pdyn*-Cre mice were used to characterize subpopulations of striatal neurons in the direct pathway (Al-Hasani et al., 2015) study D1/D2-type neuron activity balance in the nucleus accumbens (Tejeda et al., 2017), rescue MOR expression in the striatum (Cui et al., 2014) or investigate amygdala circuitry (Crowley et al., 2016). On the receptor side, one knock-in Cre line was created to gain genetic access to kappa opioid receptor (KOR)-expressing cells (X. Cai et al., 2016), and used to study peripheral KOR-neuron terminals in pain control (Snyder et al., 2018). This work provides a tool to access MOR-neurons.

Full characterization of this novel *Oprm1*-Cre driver line demonstrates that: (i) MOR signaling and function are preserved, as shown by intact G protein activation and normal morphine-induced analgesia, locomotor stimulation and sensitization, (ii) the eGFP/Cre is detectable and expression pattern matches MOR expression, and (iii) the eGFP/Cre recombinase is functional and effectively drives both the expression of Cre-dependent reporter genes and optogenetic sensors in MOR-expressing neurons. Together with a recently published inducible MOR-CreER mouse line (Okunomiya et al., 2020), this *Oprm1*-Cre line is a unique tool for both mapping and functional studies of MOR-positive neurons, and will be of broad interest for opioid, pain, reward and addiction research.

References

Al-Hasani, R., McCall, J. G., Shin, G., Gomez, A. M., Schmitz, G. P., Bernardi, J. M., Pyo, C. O., Park, S. I., Marcinkiewcz, C. M., Crowley, N. A., Krashes, M. J., Lowell, B. B., Kash, T. L., Rogers, J. A., & Bruchas, M. R. (2015). Distinct Subpopulations of Nucleus Accumbens Dynorphin Neurons Drive Aversion and Reward. *Neuron, 87*(5), 1063-1077

Cahill, C. M., Walwyn, W., Taylor, A. M. W., Pradhan, A. A. A., & Evans, C. J. (2016). Allostatic Mechanisms of Opioid Tolerance Beyond Desensitization and Downregulation. *Trends Pharmacol Sci, 37*(11), 963-976

Cai, D., Cohen, K. B., Luo, T., Lichtman, J. W., & Sanes, J. R. (2013). Improved tools for the Brainbow toolbox. *Nat Methods, 10*(6), 540-547

Cai, X., Huang, H., Kuzirian, M. S., Snyder, L. M., Matsushita, M., Lee, M. C., Ferguson, C., Homanics, G. E., Barth, A. L., & Ross, S. E. (2016). Generation of a KOR-Cre knockin mouse strain to study cells involved in kappa opioid signaling. *Genesis, 54*(1), 29-37

Charbogne, P., Gardon, O., Martin-Garcia, E., Keyworth, H. L., Matsui, A., Mechling, A. E., et al. (2017). Mu Opioid Receptors in Gamma-Aminobutyric Acidergic Forebrain Neurons Moderate Motivation for Heroin and Palatable Food. *Biol Psychiatry, 81*(9), 778-788

Contet, C., Kieffer, B. L., & Befort, K. (2004). Mu opioid receptor: a gateway to drug addiction. *Curr Opin Neurobiol, 14*(3), 370-378

Corder, G., Castro, D. C., Bruchas, M. R., & Scherrer, G. (2018). Endogenous and Exogenous Opioids in Pain. *Annu Rev Neurosci, 41*, 453-473

Crowley, N. A., Bloodgood, D. W., Hardaway, J. A., Kendra, A. M., McCall, J. G., Al-Hasani, R., McCall, N. M., Yu, W., Schools, Z. L., Krashes, M. J., Lowell, B. B., Whistler, J. L., Bruchas, M. R., & Kash, T. L. (2016). Dynorphin Controls the Gain of an Amygdalar Anxiety Circuit. *Cell Rep, 14*(12), 2774-2783

448 Cui, Y., Ostlund, S. B., James, A. S., Park, C. S., Ge, W., Roberts, K. W., Mittal, N., Murphy, N.
449 P., Cepeda, C., Kieffer, B. L., Levine, M. S., Jentsch, J. D., Walwyn, W. M., Sun, Y. E.,
450 Evans, C. J., Maidment, N. T., & Yang, X. W. (2014). Targeted expression of mu-opioid
451 receptors in a subset of striatal direct-pathway neurons restores opiate reward. *Nat*
452 *Neurosci, 17*(2), 254-261
453 Darcq, E., Befort, K., Koebel, P., Pannetier, S., Mahoney, M. K., Gaveriaux-Ruff, C., Hanauer,
454 A., & Kieffer, B. L. (2012). RSK2 signaling in medial habenula contributes to acute
455 morphine analgesia. *Neuropsychopharmacology, 37*(5), 1288-1296
456 Darcq, E., & Kieffer, B. L. (2018). Opioid receptors: drivers to addiction? *Nat Rev Neurosci,*
457 *19*(8), 499-514
458 Erbs, E., Faget, L., Scherrer, G., Matifas, A., Filliol, D., Vonesch, J. L., Koch, M., Kessler, P.,
459 Hentsch, D., Birling, M. C., Koutsourakis, M., Vasseur, L., Veinante, P., Kieffer, B. L., &
460 Massotte, D. (2015). A mu-delta opioid receptor brain atlas reveals neuronal co-
461 occurrence in subcortical networks. *Brain Struct Funct, 220*(2), 677-702
462 Fenno, L., Yizhar, O., & Deisseroth, K. (2011). The development and application of
463 optogenetics. *Annu Rev Neurosci, 34*, 389-412
464 Fields, H. L., & Margolis, E. B. (2015). Understanding opioid reward. *Trends Neurosci, 38*(4),
465 217-225
466 Gardon, O., Faget, L., Chu Sin Chung, P., Matifas, A., Massotte, D., & Kieffer, B. L. (2014).
467 Expression of mu opioid receptor in dorsal diencephalic conduction system: new insights
468 for the medial habenula. *Neuroscience, 277*, 595-609
469 Gaveriaux-Ruff, C., & Kieffer, B. L. (2007). Conditional gene targeting in the mouse nervous
470 system: Insights into brain function and diseases. *Pharmacol Ther, 113*(3), 619-634
471 Gong, S., Doughty, M., Harbaugh, C. R., Cummins, A., Hatten, M. E., Heintz, N., & Gerfen, C.
472 R. (2007). Targeting Cre recombinase to specific neuron populations with bacterial
473 artificial chromosome constructs. *J Neurosci, 27*(37), 9817-9823

474 Harris, J. A., Hirokawa, K. E., Sorensen, S. A., Gu, H., Mills, M., Ng, L. L., Bohn, P., Mortrud,
475 M., Ouellette, B., Kidney, J., Smith, K. A., Dang, C., Sunkin, S., Bernard, A., Oh, S. W.,
476 Madisen, L., & Zeng, H. (2014). Anatomical characterization of Cre driver mice for neural
477 circuit mapping and manipulation. *Front Neural Circuits, 8*, 76
478 Johnson, S. W., & North, R. A. (1992). Opioids excite dopamine neurons by hyperpolarization of
479 local interneurons. *J Neurosci, 12*(2), 483-488
480 Levitt, E. S., & Williams, J. T. (2018). Desensitization and Tolerance of Mu Opioid Receptors on
481 Pontine Kolliker-Fuse Neurons. *Mol Pharmacol, 93*(1), 8-13
482 Livak, K. J., & Schmittgen, T. D. (2001). Analysis of relative gene expression data using real-
483 time quantitative PCR and the 2(-Delta Delta C(T)) Method. *Methods, 25*(4), 402-408
484 Lutz, P. E., & Kieffer, B. L. (2013). Opioid receptors: distinct roles in mood disorders. *Trends*
485 *Neurosci, 36*(3), 195-206
486 Matthes, H. W., Maldonado, R., Simonin, F., Valverde, O., Slowe, S., Kitchen, I., Befort, K.,
487 Dierich, A., Le Meur, M., Dolle, P., Tzavara, E., Hanoune, J., Roques, B. P., & Kieffer, B.
488 L. (1996). Loss of morphine-induced analgesia, reward effect and withdrawal symptoms
489 in mice lacking the mu-opioid-receptor gene. *Nature, 383*(6603), 819-823
490 Mechling, A. E., Arefin, T., Lee, H. L., Bienert, T., Reisert, M., Ben Hamida, S., Darcq, E.,
491 Ehrlich, A., Gaveriaux-Ruff, C., Parent, M. J., Rosa-Neto, P., Hennig, J., von Elverfeldt,
492 D., Kieffer, B. L., & Harsan, L. A. (2016). Deletion of the mu opioid receptor gene in mice
493 reshapes the reward-aversion connectome. *Proc Natl Acad Sci U S A, 113*(41), 11603-
494 11608
495 Meirsman, A. C., Le Merrer, J., Pellissier, L. P., Diaz, J., Clesse, D., Kieffer, B. L., & Becker, J.
496 A. (2016). Mice Lacking GPR88 Show Motor Deficit, Improved Spatial Learning, and
497 Low Anxiety Reversed by Delta Opioid Antagonist. *Biol Psychiatry, 79*(11), 917-927
498 Nasseef, M. T., Singh, J. P., Ehrlich, A. T., McNicholas, M., Park, D. W., Ma, W., Kulkarni, P.,
499 Kieffer, B. L., & Darcq, E. (2019). Oxycodone-Mediated Activation of the Mu Opioid

500 Receptor Reduces Whole Brain Functional Connectivity in Mice. *ACS Pharmacology &*
501 *Translational Science, 2*(4), 264-274
502 Okunomiya, T., Hioki, H., Nishimura, C., Yawata, S., Imayoshi, I., Kageyama, R., Takahashi, R.,
503 & Watanabe, D. (2020). Generation of a MOR-CreER knock-in mouse line to study cells
504 and neural circuits involved in mu opioid receptor signaling. *Genesis, 58*(1), e23341
505 Pradhan, A. A., Becker, J. A., Scherrer, G., Tryoen-Toth, P., Filliol, D., Matifas, A., Massotte, D.,
506 Gaveriaux-Ruff, C., & Kieffer, B. L. (2009). In vivo delta opioid receptor internalization
507 controls behavioral effects of agonists. *PLoS One, 4*(5), e5425
508 Russell, J. T. (2011). Imaging calcium signals in vivo: a powerful tool in physiology and
509 pharmacology. *Br J Pharmacol, 163*(8), 1605-1625
510 Seo, D. O., Funderburk, S. C., Bhatti, D. L., Motard, L. E., Newbold, D., Girven, K. S., McCall, J.
511 G., Krashes, M., Sparta, D. R., & Bruchas, M. R. (2016). A GABAergic Projection from
512 the Centromedial Nuclei of the Amygdala to Ventromedial Prefrontal Cortex Modulates
513 Reward Behavior. *J Neurosci, 36*(42), 10831-10842
514 Snyder, L. M., Chiang, M. C., Loeza-Alcocer, E., Omori, Y., Hachisuka, J., Sheahan, T. D., et al.
515 (2018). Kappa Opioid Receptor Distribution and Function in Primary Afferents. *Neuron,*
516 *99*(6), 1274-1288 e1276
517 Soden, M. E., Gore, B. B., & Zweifel, L. S. (2014). Defining functional gene-circuit interfaces in
518 the mouse nervous system. *Genes Brain Behav, 13*(1), 2-12
519 Sternson, S. M., & Roth, B. L. (2014). Chemogenetic tools to interrogate brain functions. *Annu*
520 *Rev Neurosci, 37*, 387-407
521 Szymczak, A. L., Workman, C. J., Wang, Y., Vignali, K. M., Dilioglou, S., Vanin, E. F., & Vignali,
522 D. A. (2004). Correction of multi-gene deficiency in vivo using a single 'self-cleaving' 2A
523 peptide-based retroviral vector. *Nat Biotechnol, 22*(5), 589-594

524 Tan, K. R., Yvon, C., Turiault, M., Mirzabekov, J. J., Doehner, J., Labouebe, G., Deisseroth, K.,
525 Tye, K. M., & Luscher, C. (2012). GABA neurons of the VTA drive conditioned place
526 aversion. *Neuron, 73*(6), 1173-1183
527 Taniguchi, H., He, M., Wu, P., Kim, S., Paik, R., Sugino, K., Kvitsiani, D., Fu, Y., Lu, J., Lin, Y.,
528 Miyoshi, G., Shima, Y., Fishell, G., Nelson, S. B., & Huang, Z. J. (2011). A resource of
529 Cre driver lines for genetic targeting of GABAergic neurons in cerebral cortex. *Neuron,*
530 *71*(6), 995-1013
531 Tejeda, H. A., Wu, J., Kornspun, A. R., Pignatelli, M., Kashtelyan, V., Krashes, M. J., Lowell, B.
532 B., Carlezon, W. A., Jr., & Bonci, A. (2017). Pathway- and Cell-Specific Kappa-Opioid
533 Receptor Modulation of Excitation-Inhibition Balance Differentially Gates D1 and D2
534 Accumbens Neuron Activity. *Neuron, 93*(1), 147-163
535 Volkow, N. D., & Koroshetz, W. J. (2019). The role of neurologists in tackling the opioid
536 epidemic. *Nat Rev Neurol, 15*(5), 301-305
537 Weibel, R., Reiss, D., Karchewski, L., Gardon, O., Matifas, A., Filliol, D., Becker, J. A., Wood, J.
538 N., Kieffer, B. L., & Gaveriaux-Ruff, C. (2013). Mu opioid receptors on primary afferent
539 nav1.8 neurons contribute to opiate-induced analgesia: insight from conditional knockout
540 mice. *PLoS One, 8*(9), e74706
541 Williams, H. D., Trevaskis, N. L., Charman, S. A., Shanker, R. M., Charman, W. N., Pouton, C.
542 W., & Porter, C. J. (2013). Strategies to address low drug solubility in discovery and
543 development. *Pharmacol Rev, 65*(1), 315-499
544 World Health Organization. (2017). Curbing prescription opioid dependency. *Bull World Health*
545 *Organ, 95*(5), 318-319
546
547

548 **Figure legends**

549

550 **Figure 1. Intact MOR function in the *Oprm1*-Cre line. a,** Targeting strategy: a cDNA encoding
551 a functional eGFP/Cre-recombinase fusion protein is inserted in frame and upstream the stop
552 codon of the *Oprm1* gene. In addition, a T2A cleavable peptide sequence is joining *Oprm1* gene
553 to the eGFP/Cre sequence, so that the eGFP/Cre enzyme is released from the receptor upon
554 translation of the MOR-T2A-eGFP/Cre fusion protein (see KI genotyping strategy in Extended
555 Data Figure 1-1). **b,** *Oprm*1 mRNA expression levels are identical between $Oprm1^{Cre/Cre}$ and
556 $Oprm1^{+/+}$ mice. Quantification was done by RT-qPCR in samples from dorsal striatum (DS),
557 nucleus accumbens (NAc), habenula (Hb), interpeduncular nucleus (IPN), ventral tegmental
558 area/substantia nigra (VTA/SN), cerebellum (Cer), periaqueductal gray (PAG) and spinal cord
559 (SC) and shows comparable *Oprm1* transcript levels across genotypes**. c,** Confocal imaging of
560 RNAscope probes targeting *eGFP* (green) and *Oprm1* (purple) mRNAs in addition of DAPI
561 staining (blue) shows co-localization of the two transcripts in dorsal striatum sections of
562 $Oprm1^{Cre/Cre}$ mice (inset). Dashed lines delimit examples of MOR-eGFP/Cre-positive neurons.
563 Magnification: x60 with immersion oil, scale =5 µm. **d.** (Left panel) Immunohistochemistry shows
564 eGFP/Cre and MOR protein expression in the same habenular subdivisions. Coronal brain
565 sections of heterozygote $Oprm1^{Cre/+}$ mice were stained with eGFP and MOR antibodies (see
566 MOR antibody validation in Extended Data Figure 1-2) and fluorescence microscopy shows the
567 expected staining mainly in basolateral (bl) and apical (a) parts of the medial habenula (MHb).
568 Bm, basomedial, sm, stria medullaris tract, magnification: x10, scale = 50 µm. (Right, 4 panels)
569 At higher magnification (inset, basolateral part of the MHb), staining reveals nuclear DAPI (blue)
570 and eGFP/Cre (green) staining, whereas MOR staining (purple) is exclusively extranuclear
571 Magnification: x60 with immersion oil. Scale = 5 µm. Dashed lines delimit one example of MOR-
572 eGFP/Cre-positive neuron. **e.** MOR signalling is preserved in $Oprm1^{Cre/Cre}$ mice. G protein
573 activation was evaluated using [^{35}S]-GTPγS binding: DAMGO-induced G protein activation is

similar in striatal membranes from the two genotypes (n= 2 pools x 4 striatum; EC_{50}, 324 nM for *Oprm1*$^{+/+}$ and 392 nM for *Oprm*$^{KI/KI}$; E_{max}, 148 ± 7 for *Oprm1*$^{WT/WT}$ and 156 ± 11 for *Oprm1*$^{Cre/Cre}$). **f.** Locomotor sensitization of morphine is intact in *Oprm1*$^{Cre/Cre}$ mice. Mice were injected at day 1, 4, 8, 11, 14, 18 with morphine (40 mg/kg, ip). Total traveled distances recorded for 2h are comparable in *Oprm1*$^{+/+}$ and *Oprm1*$^{Cre/Cre}$ mice (n=7 animals/group). Data are presented as mean ± SEM. **g**. Analgesic effects of morphine are intact in *Oprm1*$^{Cre/Cre}$ mice. Analgesia was assessed by tail immersion test: identical tail withdrawal latencies were measured at 48°C and 52°C, in wild-type *Oprm1*$^{+/+}$ and *Oprm1*$^{Cre/Cre}$ mice 45 minutes after a single saline or morphine injection (2.5 or 5 mg/kg) (n=10 animals/group). Dashed horizontal lines show cut-off at 15 sec for 48°C and 10 sec for 52°C. Data are presented as mean ± SEM, *** $p < 0.001$ morphine effect compared to saline.

Figure 2. Cre-mediated recombination is efficient in the *Oprm1*-Cre line. a, Cre-mediated expression of the fluorescent reporter tdTomato in the habenula-interpeduncular pathway. (left) Cre recombination upon local injection of an AAV2.EF1a.DIO.mCherry viral reporter in the medial habenula (MHb) and (right) Cre recombination upon breeding Cre-dependent tdTomato reporter mice with the *Oprm1*-Cre line both lead to a strong fluorescent signal in apical (a) and basolateral (bl) of the MHb, as well as in the rostral (ipr) and lateral (ipl) areas of the interpeduncular nucleus (IPN). Scale = 100 µm. **b,** Cre-mediated tdTomato expression in the adult brain of *Oprm1*-Cre x tdTomato mice. (top) Whole brain sagittal views show high tdTomato expression in the thalamus, as well as the entire mesolimbic (left) and MHb-IPN (right) pathways. Scale = 500 µm. (middle). Coronal sections show strong fluorescence in the basal ganglia, thalamus as well as in most amygdalar nuclei with the notable exception of basolateral amygdala. Scale =500 µm. (bottom) Higher magnification highlights both cell bodies and/or fibers patterns of labelled neurons. Scale =200 µm. Slides were scanned on the Olympus VS120 (Olympus Corporation, Shinjuku, Tokyo, Japan) with a 10× objective. Abbreviations :

600 BLA, basolateral amygdala; CeA, central amygdala; DS, dorsal striatum; EP, endopiriform
601 nucleus; fr, fasciculus retroflexus; GP, globus pallidus; HIP, hippocampus; IA, intercalated
602 amygdala; LHb, lateral habenula; Nac, nucleus accumbens; OT, olfactory tubercle; SNr,
603 substantia nigra; Th, thalamus; VTA, ventral tegmental area.
604
605 **Figure 3. The *Oprm1*-Cre line is amenable to optogenetics.** *Oprm1*-Cre$^{VTA\text{-}VTA::ChR2}$
606 photostimulation causes behavioral avoidance. **a**, Diagram showing viral delivery of
607 AAV2.EF1a.DIO.ChR2-mCherry (channelorhodopsin) or AAV2.EF1a.DIO.mCherry (control) into
608 the VTA and fiber-optic implantation above the VTA, a well as a timeline for the experimental
609 procedure. **b** Representative image of viral expression (red), optic fiber implantation and VTA
610 dopamine cells immunostained with anti-Tyrosine Hydroxylase (TH)/Alexa647 (blue). Tissues
611 were observed on an inverted epifluorescence microscope. **c.** Confocal imaging of VTA sections
612 stained with GABA antibody show overlapping with viral expression. Scale = 10 µm. **d,**
613 Occupancy plots for representative individual at 20 Hz. Mice were free to explore the two-
614 chambers RTPT apparatus for 20 min. Mice then received a blue stimulation when entering the
615 light-paired side at 0, 10, 20 and 40 Hz (473nm, 10 mW, 10 ms pulse width) on four consecutive
616 days, as described by (Seo et al., 2016). **e** VTA MOR neurons activation produce place
617 avoidance. Light stimulation in *Oprm1*-Cre$^{VTA\text{-}VTA::ChR2}$ mice induced significant behavioral
618 avoidance to the light-paired side compared to control group (n 7-8/group). The graph shows
619 frequency-responses of mice receiving a blue stimulation when entering the light-paired side
620 (473nm, 10 mW, 10 ms pulse width at 0, 10, 20 and 40 Hz; n=9-10, control vs ChR2). Data are
621 expressed as mean ± SEM * $p<0.05$, ***$p<0.001$ **f**. Further analysis of the 20 Hz simulation
622 condition indicated significant avoidance for the light-paired side without affecting the total
623 distance travelled ($p>0.05$).
624

Extended Data Figure 1-1. KI genotyping strategy. Diagram describing the position of the primers used for genotyping.

Extended Data Figure 1-2. UMB3 expression and antibody validation. Coronal sections of habenula were stained with UMB3 antibody and show MOR expression in wild-type mice (left), but no signal could be detected in the MOR KO mice (right). Scale = 100 μm

Movie 1. 3D views of the whole brain.

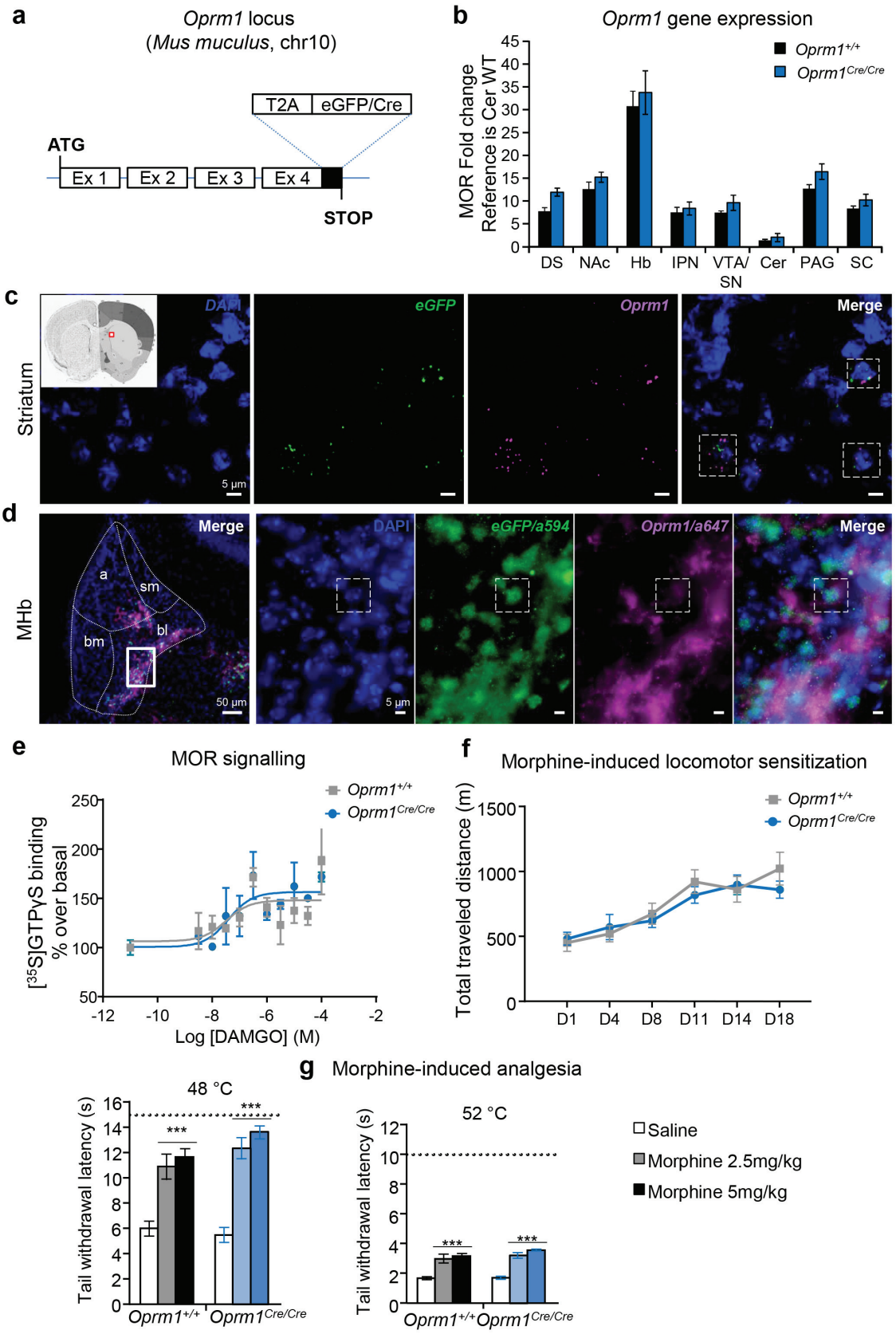

Figure 1

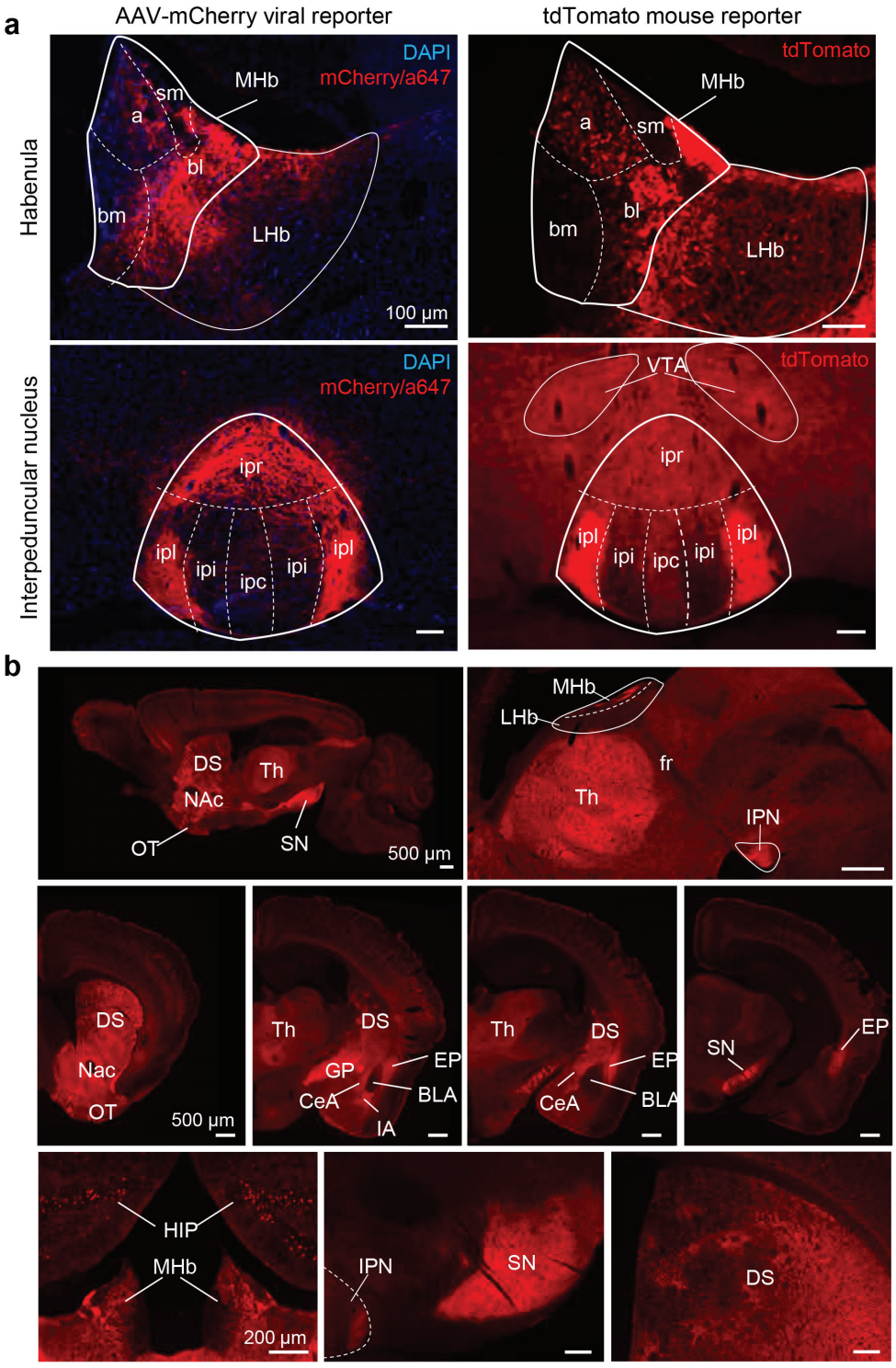

Figure 2

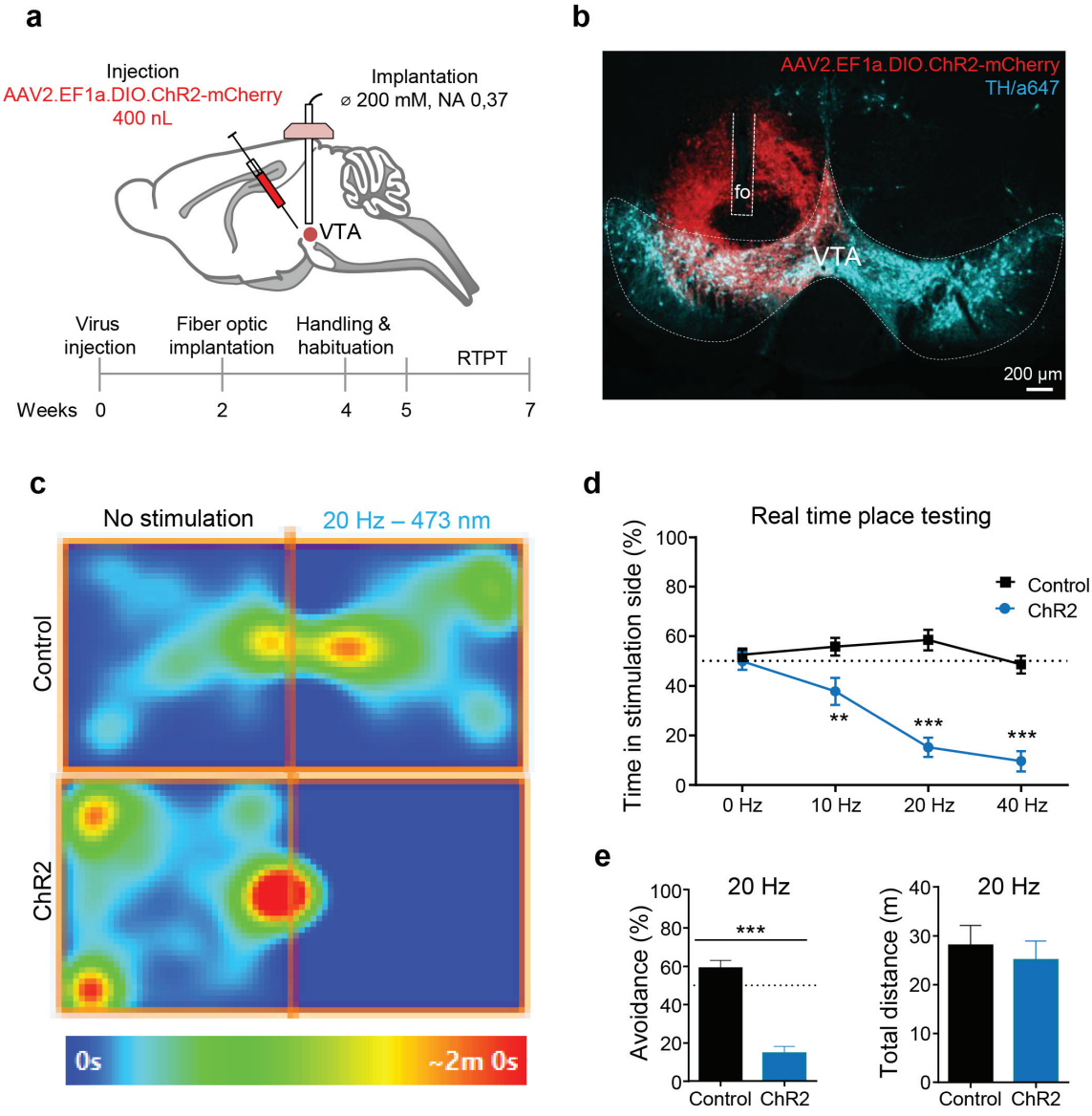

Figure 3